The similarity of magnetic ordering of these compounds to a sc Heisenberg model, then, is due to the overall three-dimensional and fairly isotropic superexchange. That the sc model falls short of an accurate physical description of these compounds is not unexpected, for the model approximates the magnetic ion as having six equivalent and equidistant nearest neighbors and does not consider such potentially important effects as further neighbor and dipole–dipole interactions. These factors, as well as the effects of additional small changes in the composition of the $A_3Fe_2X_9$ salts on structural magnetic properties including specific heat measurements and neutron spin structures, will be considered in the future, in an effort toward a better understanding of some of the fundamentals of magnetomolecular architecture.

Acknowledgment. We thank Dr. K. R. Seddon and Dr. Jalal Zora for introducing us to this series of compounds. We also thank Ramon Burriel for helpful suggestions for this manuscript. This work was supported by the Solid State Chemistry Program of the Division of Materials Research of the National Science Foundation, under Grants DMR-8515224 and DMR-8815798. Acknowledgment is made to the donors of the Petroleum Research Fund, administered by the American Chemical Society, for partial support of this research. Work at Argonne National Laboratory was sponsored by the U.S. Department of Energy, Office of Basic Energy Sciences, Division of Materials Sciences, under Contract W-31-109-Eng-38.

Supplementary Material Available: Tables of crystallographic parameters (Table S1), anisotropic thermal parameters (Tables S2 and S5), and distances and angles (Tables S3 and S6) (8 pages); tables of structure factors (Tables S4 and S7) (38 pages). Ordering information is given on any current masthead page.

Contribution from the Laboratoire de Chimie de Coordination du CNRS,† 205 route de Narbonne, 31077 Toulouse Cedex, France, and Department of Chemistry, University of Poona, Poona, 411007 India

Iron(II) Complexes of Ortho-Functionalized *p*-Naphthoquinones. 2. Crystal and Molecular Structure of Bis(aquo)bis(lawsonato)iron(II) and Intermolecular Magnetic Exchange Interactions in Bis(3-aminolawsonato)iron(II)

Prafulla Garge,[1a] Rajeev Chikate,[1a] Subhash Padhye,*[,1a] Jean-Michel Savariault,[1b] Philippe de Loth,[1b] and Jean-Pierre Tuchagues*[,1b]

Received July 11, 1989

Two related complexes [Fe(lawsonato)$_2$(H_2O)$_2$] (**1**) and [Fe(3-aminolawsonato)$_2$(CH_3OH)] (**2**), wherein lawsonato is the anion of 2-hydroxy-1,4-naphthoquinone, have been synthesized and studied. **1** crystallizes in the monoclinic system, space group $P2_1/c$ with $Z = 2$, $a = 5.036$ (3) Å, $b = 16.448$ (3) Å, $c = 10.710$ (3) Å, and $\beta = 99.75$ (4)°. The structure was solved by the heavy-atom method and refined to conventional agreement indices $R = 0.051$ and $R_w = 0.057$ with 1444 unique reflections for which $I > 2\sigma$. The three-dimensional network of the crystal results from the linking of infinite chains of [Fe(lawsonato)$_2$(H_2O)$_2$] molecules through hydrogen bonds. These chains consist of complex molecules doubly hydrogen-bonded along the [100] direction. Each complex molecule comprises two bidentate lawsone ligands coordinated to the ferrous iron center in their fully oxidized *p*-quinone form and two trans water molecules. The resulting coordination sphere can be described as a rhombically distorted octahedron. The synthesis, IR, UV–visible, and Mössbauer spectra, and thermogravimetric, variable-temperature magnetic susceptibility, and cyclic voltammetry studies of **2** are described. Both 3-aminolawsone ligands are in their fully oxidized form, and the coordinating centers are the C(2) phenolate oxygen and C(3) amino nitrogen atoms. Variable-temperature magnetic susceptibility studies establish the presence of isotropic magnetic exchange interactions between the high-spin iron(II) centers of a dimeric species ($J = -1.6$ cm^{-1}) and crystalline field anisotropy of the ferrous ion ($D = 4.9$ cm^{-1}). The dimeric structural arrangement of **2** implies a N_2O_4 ligand environment holding two *p*-naphthoquinone moieties at ca. 4 Å from the ferrous center and can therefore serve as a basis for studying the effect of quinone oxidation state changes on electronic and magnetic properties of the iron(II)–quinone couple in the "ferroquinone complex" of photosynthetic bacteria and photosystem 2.

Introduction

Quinones play an integral role in many biological electron-transfer processes, particularly respiration and photosynthesis.[2] Some of these reactions are catalyzed by metal ions like copper, iron, manganese, and molybdenum, although mechanistic aspects of these interactions have not been fully elucidated.[3] During these processes, quinones are reversibly reduced to either semiquinone radical anions or dianionic catechols with concomitant oxidation of the divalent metal ions.

Studies on ubiquinones have shown that they function as electron shuttles between various flavoprotein dehydrogenases in the electron-transport chain.[4] Similarly, plastoquinones and catechols are known to be involved in green plants and enzymatically catalyzed reactions of oxygen.[5] In view of the roles of quinones in electron-transport chains, it is important to characterize and thoroughly study metal complexes with quinone derivatives of biological relevance. For this purpose, hydroxyquinone ligands of natural occurrence have been studied for some time.[6] More recently, we have reported on the mononuclear iron(II) complexes of ortho-functionalized *p*-naphthoquinones, showing that the bound quinone ligands are in their fully oxidized form.[7]

In the present paper, the molecular crystal structure of one such high-spin ferrous complex of lawsone is described for the first time. Lawsone is the 2-hydroxy-1,4-naphthoquinone pigment found in

† Unité No. 8241 liée par conventions à l'Université Paul Sabatier et à l'Institut National Polytechnique de Toulouse.

(1) (a) University of Poona. (b) Laboratoire de Chimie de Coordination du CNRS.
(2) (a) Thomson, R. H. *Naturally Occurring Quinones*; Academic Press: New York, 1971. (b) Morton, R. A. *Biochemistry of Quinones*; Academic Press: New York, 1965.
(3) Buchanan, R. M.; Pierpont, C. G. *Coord. Chem. Rev.* **1981**, *38*, 45–87.
(4) (a) Orme-Johnson, N. R.; Orme-Johnson, W. H.; Hansen, R. E.; Beinert, H.; Hatefi, Y. *Biochem. Biophys. Res. Commun.* **1971**, *44*, 446–452. (b) Tikhonov, A. N.; Burvaev, D. S.; Grigolva, I. V.; Konstantinov, A. A.; Kzenzenko, M. Y.; Ruug, E. *Biofizika* **1977**, *22*, 734–736. (c) Ruzicka, F. J.; Beinert, H.; Schepler, K. L.; Dunham, W. R.; Sands, R. H. *Proc. Natl. Acad. Sci. U.S.A.* **1975**, *72*, 2886–2890. (d) Konstantinov, A. A.; Ruug, E. *Bioorg. Khym.* **1977**, *3*, 787–799.
(5) (a) Feher, G.; Isaacson, R. A.; McElroy, J. D.; Ackerson, I. E.; Okamura, M. Y. *Biochim. Biophys. Acta* **1974**, *368*, 135–139. (b) Wraight, C. A. *FEBS Lett.* **1978**, *93*, 283–287. (c) Govindjee, Ed. *Bioenergetics of Photosynthesis*; Academic Press: New York, 1974.
(6) (a) Padhye, S. B.; Kulkarni, B. A. *J. Phys. Chem.* **1975**, *79*, 927–928. (b) Padhye, S. B.; Kulkarni, B. A. *J. Magn. Res.* **1974**, *16*, 150–152.
(7) (a) Padhye, S.; Garge, P.; Gupta, M. P. *Inorg. Chim. Acta* **1988**, *152*, 37–42. (b) Garge, P.; Padhye, S.; Tuchagues, J. P. *Inorg. Chim. Acta* **1989**, *157*, 239–249.

0020-1669/90/1329-3315$02.50/0

Table I. Crystallographic Data for $[Fe(lawsonato)_2(H_2O)_2]$ (**1**)

formula of the asymmetric unit	$C_{20}H_{14}O_8Fe$
fw	438.18
a, Å	5.036 (3)
b, Å	16.448 (3)
c, Å	10.710 (3)
β, deg	99.75 (4)
V, Å^3	874.4 (1)
space group	$P2_1/c$
Z	2
d_{obsd}, g·cm^{-3}	1.59 (3)
d_{calcd}, g·cm^{-3}	1.66
T, K	295
radiation (graphite monochromator, Mo Kα): λ, Å	0.71069
μ(Mo Kα), cm^{-1}	9.07
$R = \sum\|k\|F_o\| - \|F_c\|\|/\sum k\|F_o\|$	0.051
$R_w = [\sum w(k\|F_o\| - \|F_c\|)^2/\sum wk^2F_o^2]^{1/2}$	0.057

the leaves of *Lawsonia alba*.[8] We also describe the synthesis and study of a new high-spin ferrous complex containing two 3-aminolawsone bidentate ligands coordinated through the 2-hydroxo and 3-amino substituents. It has been shown that several complexes containing planar quinone ligands experience strong intermolecular interactions, which result in magnetic moments well below the ground-state moment.[3] For example, the iron and molybdenum complexes prepared with 9,10-phenanthrenequinone as a ligand have been found to involve stacked structures exhibiting intermolecular magnetic exchange interactions.[9]

The results of an investigation on the magnetic properties of the above mentioned 3-aminolawsone complex of iron(II) are also presented in this paper.

Experimental Section

The synthesis of $[Fe(lawsonato)_2(H_2O)_2]$ (**1**) has been described in a previous paper.[7b] Crystals of this complex suitable for X-ray measurements were grown by slow evaporation of a methanolic solution of the compound.

3-Aminolawsone was prepared from 3-nitrolawsone by reduction with sodium dithionite using a reported procedure.[10] A careful purification of the resulting crude compound by crystallization from aqueous acetic acid (pH 5) followed by sublimation at 70 °C under vacuum (0.01 mmHg) was necessary to obtain the pure 3-aminolawsone ligand.

The corresponding ferrous complex, $[Fe(3\text{-aminolawsonato})_2(CH_3OH)]$ (**2**), was prepared by mixing the degassed solutions of $FeSO_4 \cdot 7H_2O$ (1 mmol, 25 mL of water) and the ligand (2 mmol, 100 mL of methanol) in a Schlenk assembly maintained under nitrogen. The final pH was adjusted between 5 and 6 with a few drops of degassed sodium acetate solution. The resulting complex (violet-blue powder) was washed with water and cold methanol and dried under vacuum. Anal. Calcd for $C_{21}H_{16}N_2O_7Fe$: C, 54.33; H, 3.45; N, 6.04; Fe, 12.04. Found: C, 54.13; H, 3.21; N, 5.84; Fe, 11.87.

The details of the physical measurements carried out on this complex are identical with those described elsewhere.[7b]

X-ray Crystal Structure Determination of $[Fe(lawsonato)_2(H_2O)_2]$ (1). Crystals of complex **1** belong to the monoclinic system, space group $P2_1/c$. The selected crystal was a black needle of approximate dimensions 0.1 × 0.1 × 0.4 mm. It was sealed on a glass fiber and mounted on an Enraf-Nonius CAD4 diffratometer. Cell constants were obtained from a least-squares fit of 25 reflections. Crystal and intensity collection data are summarized in Table I. A total of 2876 reflections were recorded to a 2θ(Mo) maximum of 60° by procedures described elsewhere.[11] Intensity standards, recorded periodically, showed no significant variations during measurements. Reflections were corrected for Lorentz and polarization effects;[12] 1444 of these reflections with $I > 2\sigma$ were used in subsequent calculations. Empirical absorption corrections were made.

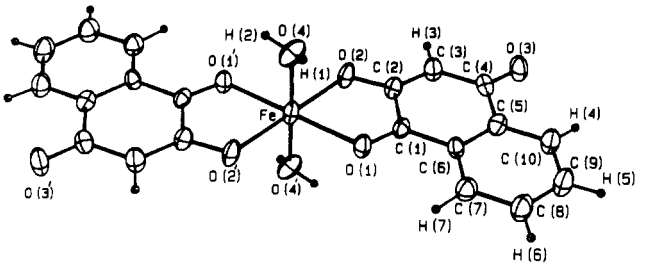

Figure 1. ORTEP view of the $[Fe(lawsonato)_2(H_2O)_2]$ molecule (**1**).

Table II. Fractional Atomic Coordinates and Isotropic Thermal Parameters for $[Fe(lawsonato)_2(H_2O)_2]$ (**1**) with Estimated Standard Deviations in Parentheses

atom	x/a	y/b	z/c	B_{iso}, Å^2[a]
Fe	0.0000	0.0000	0.0000	2.10 (2)
O(1)	0.1366 (6)	0.1229 (2)	−0.0100 (3)	2.36 (7)
O(2)	−0.1944 (7)	0.0571 (2)	0.1282 (3)	2.66 (8)
O(3)	−0.3318 (7)	0.3151 (2)	0.2917 (4)	3.11 (8)
O(4)	0.3390 (8)	−0.0210 (2)	0.1469 (4)	3.16 (9)
C(1)	0.0331 (9)	0.1696 (2)	0.0584 (4)	1.90 (8)
C(2)	−0.1565 (9)	0.1351 (3)	0.1389 (5)	2.14 (9)
C(3)	−0.269 (1)	0.1851 (3)	0.2156 (5)	2.6 (1)
C(4)	−0.2186 (9)	0.2714 (3)	0.2224 (5)	2.31 (9)
C(5)	−0.0302 (9)	0.3072 (3)	0.1434 (5)	2.20 (9)
C(6)	0.0874 (9)	0.2575 (3)	0.0609 (4)	1.96 (8)
C(7)	0.260 (1)	0.2901 (3)	−0.0148 (5)	2.6 (1)
C(8)	0.312 (1)	0.3729 (3)	−0.0086 (6)	3.2 (1)
C(9)	0.202 (1)	0.4216 (3)	0.0745 (6)	3.4 (1)
C(10)	0.033 (1)	0.3894 (3)	0.1500 (5)	2.8 (1)
H(1)	0.47 (1)	0.002 (4)	0.145 (5)	3.9 (5)*
H(2)	0.36 (1)	−0.068 (4)	0.166 (6)	3.9 (5)*
H(3)	−0.40 (1)	0.162 (3)	0.267 (5)	3.9 (5)*
H(4)	−0.06 (1)	0.422 (3)	0.200 (5)	6.08*
H(5)	0.24 (1)	0.476 (3)	0.081 (5)	6.08*
H(6)	0.43 (1)	0.395 (3)	−0.057 (5)	6.08*
H(7)	0.33 (1)	0.258 (3)	−0.077 (5)	6.08*

[a] Starred values indicate hydrogen atoms refined with a fixed isotropic thermal parameter. Anisotropically refined atoms are given in the form of the isotropic equivalent displacement parameter defined as $^4/_3[a^2B(1,1) + b^2B(2,2) + c^2B(3,3) + ac(\cos\beta)B(1,3)]$, where a, b, c, and β are reciprocal cell parameters.

Structure Solution and Refinement. The structure was solved by using the heavy-atom method.[13] The iron atom lying on a crystallographic inversion center, the refinement was carried out with half a molecule. A succession of difference Fourier syntheses and least-squares refinements revealed the positions of all atoms including the hydrogens. All non-hydrogen atoms were refined anisotropically. All hydrogen atoms were included in the calculations with a mean isotropic temperature factor U = 0.077 Å^2. The atomic scattering factors used were those proposed by Cromer and Waber[14] with anomalous dispersion effects.[15] The final full-matrix least-squares refinement, minimizing $\sum w(|F_o| - |F_c|)^2$, converged to $R = \sum||F_o| - |F_c||/\sum|F_o| = 0.051$ and $R_w = [\sum w(|F_o| - |F_c|)^2/\sum w|F_o|^2]^{1/2} = 0.057$ with a weighting scheme $w = 1$. A different weighting scheme did not improve the refinement according to the Hamilton test.[16] The goodness of fit was $s = 1.25$ with 1444 observations and 154 variables.

All calculations were performed on a VAX 11/730 DEC computer using the programs SDP,[12] SHELX 76,[17] SHELX 86,[13] and ORTEP.[18] The $[Fe(lawsonato)_2(H_2O)_2]$ molecule is shown in Figure 1 with atom num-

(8) (a) Lal, J. B.; Dutt, S. *J. Indian Chem. Soc.* **1933**, *10*, 577–582. (b) Reference 2b, p 356.
(9) (a) Pierpont, C. G.; Buchanan, R. M. *J. Am. Chem. Soc.* **1975**, *97*, 4912–4917. (b) Pierpont, C. G.; Buchanan, R. M. *J. Am. Chem. Soc.* **1975**, *97*, 6450–6455. (c) Buchanan, R. M.; Kessel, S. C.; Downs, H. H.; Pierpont, C. G.; Hendrickson, D. N. *J. Am. Chem. Soc.* **1978**, *100*, 7894–7900.
(10) Nagase, Y.; Matsumoto, U. *Yakugaku Zasshi* **1961**, *81*, 627–630.
(11) Mosset, A.; Bonnet, J.-J.; Galy, J. *Acta Crystallogr., Sect. B: Struct. Crystallogr. Cryst. Chem.* **1977**, *B33*, 2639–2644.
(12) Frenz, B. A. *SDP-Structure Determination Package*; Enraf–Nonius: Delft, Holland, 1982.
(13) Sheldrick, G. M. In *Crystallographic Computing 3*; Sheldrick, G. M., Krüger, C., Goddard, R., Eds.; Oxford University Press: Oxford, England, 1985; p 175–179.
(14) Cromer, D. T.; Waber, J. T. *International Tables for X-ray Crystallography*; Kynoch Press: Birmingham, England, 1974; Vol. IV, Table 2.2.B, pp 99, 101.
(15) Cromer, D. T. *International Tables for X-ray Crystallography*; Table 2.3.1., p 149.
(16) Hamilton, W. C. *Acta Crystallogr., Sect. B: Struct. Crytallogr. Cryst. Chem.* **1965**, *18*, 502–510.
(17) Sheldrick, G. M. *SHELX 76. Program for Crystal Structure Determination*; University of Cambridge: Cambridge, England, 1976.
(18) Johnson, C. K. ORTEP. Report ORNL-1794; Oak Ridge National Laboratory: Oak Ridge, TN, 1965.

Table III. Interatomic Distances (Å) and Bond Angles (deg) for [Fe(lawsonato)$_2$(H$_2$O)$_2$] (**1**) with Estimated Standard Deivations in Parentheses[a]

	Iron Environment		
Fe–O(1)	2.143 (4)	O(1)–Fe–O(2)	101.9 (1)
Fe–O(2)	2.045 (4)	O(1)–Fe–O(4)	88.1 (1)
Fe–O(4)	2.145 (4)	O(2)–Fe–O(4)	90.4 (1)
	Ligand		
O(1)–C(1)	1.236 (6)	O(2)–C(2)	1.298 (6)
O(3)–C(4)	1.239 (6)	C(1)–C(6)	1.471 (6)
C(1)–C(2)	1.502 (7)	C(3)–C(4)	1.443 (6)
C(2)–C(3)	1.354 (8)	C(3)–H(3)	1.00 (6)
C(4)–C(5)	1.494 (8)	C(5)–C(6)	1.406 (7)
C(5)–C(10)	1.389 (6)	C(6)–C(7)	1.393 (7)
C(7)–C(8)	1.386 (8)	C(7)–H(7)	0.96 (6)
C(8)–C(9)	1.381 (9)	C(8)–H(6)	0.92 (6)
C(9)–C(10)	1.377 (9)	C(9)–H(5)	0.92 (5)
C(10)–H(4)	0.94 (6)	O(2″)–O(4)	2.716 (5)
O(3‴)–O(4)	2.777 (5)	H(1)–O(2″)	1.94 (7)
H(1)–O(4)	0.78 (6)	H(2)–O(3‴)	1.99 (6)
H(2)–O(4)	0.79 (7)		
O(1)–C(1)–C(6)	121.7 (4)	O(1)–C(1)–C(2)	118.6 (4)
O(2)–C(2)–C(1)	115.0 (5)	O(2)–C(2)–C(3)	125.7 (5)
O(3)–C(4)–C(5)	120.8 (5)	O(3)–C(4)–C(3)	120.3 (5)
C(1)–C(2)–C(3)	119.4 (4)	C(1)–C(2)–C(6)	119.7 (4)
C(1)–C(6)–C(5)	119.0 (4)	C(1)–C(6)–C(7)	120.0 (4)
C(2)–C(3)–H(3)	119.0 (3)	C(2)–C(3)–C(4)	122.8 (5)
C(3)–C(4)–C(5)	118.8 (4)	C(4)–C(3)–H(3)	118.0 (3)
C(4)–C(5)–C(6)	120.2 (4)	C(4)–C(5)–C(10)	121.0 (4)
C(5)–C(6)–C(7)	121.0 (5)	C(5)–C(10)–C(9)	120.2 (5)
C(5)–C(10)–H(4)	117.0 (4)	C(6)–C(5)–C(10)	118.7 (5)
C(6)–C(7)–C(8)	118.7 (5)	C(6)–C(7)–H(7)	121.0 (3)
C(7)–C(8)–C(9)	120.6 (6)	C(7)–C(8)–H(6)	119.0 (4)
C(8)–C(7)–H(7)	120.0 (3)	C(8)–C(9)–H(5)	122.0 (4)
C(8)–C(9)–C(10)	120.7 (5)	C(9)–C(8)–H(6)	121.0 (4)
C(9)–C(10)–H(4)	122.0 (3)	C(10)–C(9)–H(5)	118.0 (4)
H(1)–O(4)–H(2)	113.0 (7)	O(2″)–H(1)–O(4)	176.0 (5)
O(3‴)–H(2)–O(4)	169.0 (6)		

[a] The prime, double primes, and triple primes, respectively, indicate the atomic equivalent positions through the following symmetry operations: $-x, -y, -z$; $1-x, -y, -z$; $-x, -^1/_2+y, ^1/_2-z$.

bering. Final fractional atomic coordinates with their estimated standard deviations and bond lengths and angles are given in Tables II and III, respectively. Complete crystal data and experimental details, components of the anisotropic temperature factors, deviations of atoms from their least-squares planes, and observed and calculated structure factor amplitudes are deposited as supplementary material.

Results and Discussion

Molecular Structure of 1. The complex molecule shown in Figure 1 is located about a crystallographic inversion center in the unit cell. Each molecule includes two trans lawsone bidentate ligands coordinated through the O(1) quinone carbonyl and O(2) phenoxy oxygen donors and two trans water molecules.

The iron ligand environment can be described as a rhombically distorted octahedron, the basal plane of which includes the O(1) and O(1′) quinone carbonyl and O(4) and O(4′) water oxygen atoms, 2.143 (3) and 2.145 (4) Å away from the iron center, respectively. The O(2) and O(2′) phenoxy oxygen donors situated at the apices are separated from the iron atom by a distance of 2.045 (4) Å. This situation results in a slightly compressed octahedron. Furthermore, the small O(1)···O(2) bite of the lawsone chelate tilts the O(2)–O(2′) axis ca. 12° from the normal to the basal plane. The equations of the coordination planes and quinone ligand plane are given as supplementary material.

The quinone C–O bond lengths in **1** are 1.237 (6) Å for C(1)–O(1) and 1.239 (6) Å for C(4)–O(3), respectively. These features are similar to the structural parameters available in the literature for the pyridine adducts of copper and manganese complexes of lawsone derivatives. However, in the later compounds there are significant differences between the C(1)—O(1) and C(4)—O(3) bond lengths, the maximum variation being observed in the bis(pyridine) adduct of the manganese complex of methyllawsone reported by Pierpont et al.,[19] where quinone

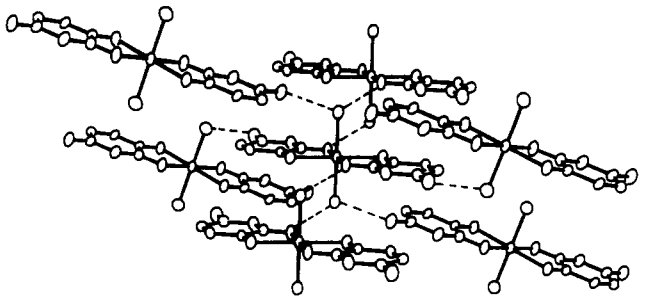

Figure 2. Perspective view of seven [Fe(lawsonato)$_2$(H$_2$O)$_2$] molecules showing the eight hydrogen bonds associated with a central molecule (dotted lines). For clarity, the benzene rings of the lawsone ligands have been omitted.

C=O bond lengths are found to be 1.217 Å for C(1)—O(1) and 1.240 Å for C(4)—O(3), respectively. A similar trend is noted in the case of the pyridine adduct of copper lawsonate.[20] In both complexes, the delocalization is found to be limited over the O(2)–C(2)–C(3)–C(4)–O(3) region of the ligand, while in the present ferrous complex it seems to extend from O(1) to O(3). The C(1)–O(1) bond lengths observed for the three complexes discussed above are significantly shorter than the C–O distances reported for a number of transition-metal complexes including either semiquinone (1.27–1.30 Å) or catecholate (1.34–1.36 Å) chelating anions.[9c,21] This observation clearly confirms that the lawsone bidentate ligands of complex **1** are involved in their fully oxidized quinone form. The C(2)–O(2) phenoxy distance of 1.298 (5) Å is equal to that reported for the similar C–O phenoxy bond in [Mn(methyllawsonato)$_2$(pyridine)$_2$][19] and also appears to reflect the conjugation over this region of the ligand.

Each [Fe(lawsonato)$_2$(H$_2$O)$_2$] molecule is linked to six neighboring molecules through eight hydrogen bonds based on the water O(4), phenoxy O(2), and quinone O(3) oxygen atoms as shown in Figure 2. Four of these hydrogen bonds involve O(4), H(1), and O(2) with a 2.716 (5) Å O(4)···O(2) distance, while the four others involve the O(4), H(2), and O(3) atoms with a 2.777 (5) Å O(4)···O(3) distance. Both distances indicate that the hydrogen bonds operating between adjacent molecules in the unit cell are strong enough to result in a close packing of the molecules. The O(4)–H(1)···O(2) contacts afford doubly hydrogen-bonded infinite chains along [100], while the O(4)–H(2)···O(3) contacts link these infinite chains together, thus affording the observed three-dimensional network. This packing results in Fe···Fe distances of 5.036 (3) Å along [100], the next closest Fe···Fe distances being 9.814 (4) Å. A stereoview of the unit cell showing the three-dimensional packing of the molecules is included in the supplementary material.

Comparative Study of Complexes 1 and 2. As evidenced from a detailed study of its properties[7b] and the above described crystal structure, **1** consists of an Fe(II) ion with an O$_6$ ligand environment comprising two bidentate lawsone ligands in their *p*-quinone tautomeric form and two water molecules. Although the lawsone ligands are in their fully oxidized quinone form, the ferrous state of the iron center is retained, as indicated by the magnetic susceptibility and Mössbauer data.[7b] As already reported, the variable-temperature magnetic susceptibility data of **1** do not indicate

(19) Mulay, M. P.; Garge, P. L.; Padhye, S. B.; Haltiwanger, R. C.; de-Learie, L. A.; Pierpont, C. G. *J. Chem. Soc., Chem. Commun.* **1987**, 581–582.

(20) Peng, S. M.; Wang, Y.; Chang, H. R.; Tang, C. P.; Wang, C. J. *Proc. Natl. Sci. Counc., Repub. China, Part B: Basic Sci.* **1981**, *5*, 139-144.

(21) (a) Buchanan, R. M.; Pierpont, C. G. *J. Am. Chem. Soc.* **1980**, *102*, 4951–4957. (b) Lynch, M. W.; Buchanan, R. M.; Pierpont, C. G.; Hendrickson, D. N. *Inorg. Chem.* **1981**, *20*, 1038–1046. (c) Lynch, M. W.; Hendrickson, D. N.; Fitzgerald, B. J.; Pierpont, C. G. *J. Am. Chem. Soc.* **1984**, *106*, 2041–2049. (d) Larsen, S. K.; Pierpont, C. G.; DeMunno, G.; Dolcetti, G. *Inorg. Chem.* **1986**, *25*, 4828–4831. (e) Linstead, M. M.; Power, P. P.; Sigel, G. A. *Inorg. Chem.* **1988**, *27*, 580–583 and references therein. (f) Boone, S. R.; Purser, G. H.; Chang, H. R.; Lowery, M. D.; Hendrickson, D. N.; Pierpont, C. G. *J. Am. Chem. Soc.* **1989**, *111*, 2292–2299.

the presence of intermolecular magnetic interactions. This is noteworthy in view of the hydrogen-bond network described in the previous section and more particularly the 5.04 Å Fe···Fe separation along [100] due to the short O(4)–H(1)···O(2) contact. In accordance with the structural determination, thermal studies indicate that both water molecules of **1** are coordinated and that their loss leads to the decomposition of the complex.[7b]

3-Aminolawsone (L) has four potential sites for binding a metal ion. The analysis of its blue ferrous complex, **2**, yields a $[M(L)_2(CH_3OH)]$ composition different from that of **1** and the other complexes in the series.[7b] Complex **2** exhibits poor solubility even in polar solvents like ethanol, DMF, and DMSO, which indicates the presence of strong intermolecular associations in the solid state. The conductivity measurements in methanol and acetonitrile reveal a nonelectrolyte behavior. All the attempts made to grow single crystals suitable for X-ray diffraction measurements were unsuccessful.

The infrared spectra of the ligand show a broad absorption around 3490 cm^{-1}, indicating that the C(2) hydroxyl group is intermolecularly hydrogen-bonded.[22] The two bands located at 3380 and 3330 cm^{-1} correspond to the symmetric and antisymmetric stretching modes of the NH_2 chromophore. On complexation, the former absorption disappears while the latter are shifted downward (3323 and 3246 cm^{-1}), which indicates that the C(2) hydroxyl and C(3) amino groups are involved in the coordination. This behavior is strikingly different from that of the other ortho-functionalized *p*-naphthoquinones which undergo coordination through the C(2) hydroxyl and C(1) carbonyl oxygen atoms.[7b] The OH absorption of the coordinated methanol molecule is located at 3440 cm^{-1}.

In the double-bond region the complex shows the split carbonyl absorption at 1628 and 1603 cm^{-1}, which corresponds to a downward shift of ca. 40 cm^{-1} compared to that of the parent ligand. This shift falls in the normal range observed for coordination in the fully oxidized quinone form. The C=C skeletal in-plane vibrations of the conjugated aromatic ring are located at 1572 and 1543 cm^{-1}, while the deformation mode of the hydroxyl stretch of the coordinated methanol molecule can be seen at 1142 cm^{-1}.[23] The ν_{C-O} frequency observed at ca. 1139 cm^{-1} in the ligand is found to undergo an upward shift (~60 cm^{-1}) on complexation, indicating an increase in the bond order and confirming the participation of the C(2) oxygen atom in the coordination. ν_{M-O} frequencies are observed at 524 and 352 cm^{-1}, which are probably coupled to ligand vibrations. The additional vibration at 488 cm^{-1} can be attributed to ν_{M-N}, as suggested by Nakamoto and Condrate.[24]

The TG/DTA profile of **2** indicates that the methanol molecule associated with the complex is lost in the 70–110 °C temperature range. It is interesting to note that such results are at variance with earlier studies on related complexes of the lawsone series having the same general formula.[7b] The loss of the coordinate methanol molecule leads to the decomposition of the chelate structure, as indicated by an accelerated loss in the TG curve. The higher decomposition temperature derived from the 120–160 °C region of the curve for **2** suggests that a more stable chelate structure is generated by the donor set of the aminolawsone ligand compared to the O_6 donor set of the other complexes in the lawsone series.

The room-temperature magnetic moment of **2** (5.12 μ_B/Fe) is slightly higher than the spin-only value of 4.9 μ_B for $S = 2$, as usually observed for high-spin iron(II) complexes, and decreases regularly to 1.65 μ_B at 4.2 K, showing the presence of antiferromagnetic interactions in the solid state.

On the grounds of the analytical, IR, and magnetic susceptibility results already described, it is clear that **2** is structurally and magnetically different from **1**. While **1** is characterized by

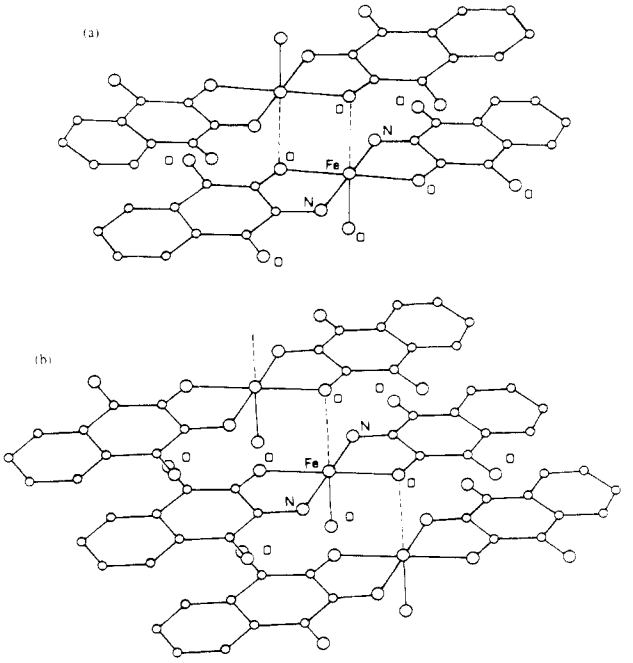

Figure 3. Schematic representation of the possible structural arrangements of $[Fe(3\text{-aminolawsonato})_2(CH_3OH)]$ (**2**): (a) dimeric species; (b) infinite chains.

magnetically isolated mononuclear ferrous complex molecules involving an O_6 donor set, **2** displays antiferromagnetically coupled molecules involving either a N_2O_3 or N_2O_4 donor set. Consquently, a detailed analysis of the magnetic properties of **2** has been carried out in order to gain some insight into its structural arrangement through magneto–structural correlations.

Considering the $[Fe(L)_2(CH_3OH)]$ mononuclear building unit of **2**, two types of structural associations can be envisaged that could result in an exchange-coupled system: the association of two mononuclear molecules should afford magnetically isolated or weakly interacting dimeric species (Figure 3a), while infinite chains would result from the association of a large number of mononuclear molecules (Figure 3b).

In order to distinguish between these possibilities, the experimental variation of the magnetic susceptibility with temperature has been tentatively analyzed within the framework of four models: (i) The least-squares fit of the experimental data to the temperature-dependent molar magnetic susceptibility expressed according to the equation for isotropic exchange in a $S_1 = S_2 = 2$ dimer,[25] modified to allow admixture of paramagnetic impurity, afforded $J = -1.94$ cm^{-1}, $g_{av} = 2.143$, and paramagnetic impurity = 0.0%. Although the fit obtained for these values was good in the high-temperature range, it was poor below 40 K. (ii) The least-squares fit of the experimental data to the temperature-dependent molar magnetic susceptibility expressed as in i and modified to take into account interdimer interactions in the molecular field approximation according to Ginsberg and Lines' approach[26] afforded poorer results. (iii) The interpretation of the variation of the experimental magnetic susceptibility with temperature was then attempted by using the magnetic susceptibility equation for a Heisenberg-type chain[27] without affording any acceptable result.

The inability of the three methods to account for the experimental results indicates that the antiferromagnetic behavior of **2** cannot be interpreted by considering only isotropic exchange interactions. Most ferrous complexes are of low enough symmetry that the ground state is orbitally nondegenerate, leaving the spin degeneracy of the $S = 2$ ion. In the presence of an axial distortion, second-order spin–orbit coupling with the orbital excited states

(22) Gaultier, J.; Hauw, C. *Acta Crystallogr., Sect. B: Struct. Crystallogr. Cryst. Chem.* **1969**, *B25*, 546–548.
(23) Nakamoto, K. *Infrared Spectra of Inorganic and Coordination Compounds*, 2nd ed.; John Wiley & Sons: New York, 1965; p 69.
(24) Condrate, R. A.; Nakamoto, K. *J. Chem. Phys.* **1965**, *42*, 2590–2598.
(25) O'Connor, C. J. *Prog. Inorg. Chem.* **1982**, *29*, 203–283.
(26) Ginsberg, A. P.; Lines, M. E. *Inorg. Chem.* **1972**, *11*, 2289–2290.
(27) (a) Fisher, M. E. *Am. J. Phys.* **1964**, *32*, 343–346. (b) König, E.; Desai, V. P. Kanellakopoulos, B.; Klenze, R. *Chem. Phys.* **1980**, *54*, 109–113.

causes the spin quintet to split. With an axial compression, the zero-field-splitting (ZFS) parameter D is positive, while it is negative for an axial elongation.[28] At low temperature, magnetic susceptibility can distinguish these cases and can be fit to give the value of D which can be as large as 15 cm^{-1} in nearly octahedral ferrous complexes.[29] The exchange-coupling constant J is known to range from positive values of a few reciprocal centimeters to values of -15 cm^{-1} for iron(II) complexes.[30] When J is much larger or smaller than D, exchange coupling or ZFS will dominate and the system can be treated as the limiting binuclear or mononuclear case, with the smaller term being at most a perturbation. However, the crystalline field anisotropy and the magnetic exchange interactions are often of the same order of magnitude in iron(II) exchange-coupled systems, leading to a complicated energy diagram.[28b,31] This situation has been treated by Kennedy and Murray[28b] and Reem and Solomon.[31b]

Considering that the least-squares fit of the experimental data to the equations for models ii and iii were poor, while that to the equation for isotropic exchange in a $S_1 = S_2 = 2$ dimer (i) was acceptable except in the low-temperature range, we finally attempted (model iv) to fit the experimental data to the theoretical magnetic susceptibility[32] calculated by exact diagonalization of the effective spin Hamiltonian taking into account the single-ion and dipolar zero-field-splitting terms.[33,34] The least-squares fitting of the experimental data to the theoretical magnetic susceptibility calculated from this model affords the solid lines drawn in Figure 4, which can be seen to approximate very well the experimental values. The parameters used to obtain the theoretical curves are $J = -1.6$ cm^{-1}, $D = 4.9$ cm^{-1}, $g_\parallel = 2.296$, $g_\perp = 2.023$, and paramagnetic impurity = 0.0%. Setting the dipolar zero-field-splitting term D_i to any value between 0 and 0.01 cm^{-1} (the maximum reasonable value for a dimer involving oxygen-bridged metal centers) did not noticeably modify the fit. The values obtained for the J, D, $g_\parallel$, and $g_\perp$ parameters fall within the range of those previously observed for iron(II) dimeric species.[30]

These results indicate that the antiferromagnetic interactions present in this compound are better approximated by the hypothesis of magnetically isolated dimeric species. The absolute value obtained for D clearly indicates that the magnetic behavior of **2** is relevant to the case where the ZFS of the single ion is of the order of magnitude of the exchange integral and cannot be treated as a perturbation. The fact that a reasonable fit could only be obtained for a positive D value indicates that the axial distortion of the ligand environment of the iron must be a compression; in these regards, it is interesting to notice that the distortion observed for the coordination octahedron of the iron in **1** is an axial compression (vide supra). Finally, these results indicate that the mononuclear molecules of **2** are most probably associated in dimeric species in the solid state as depicted in Figure 3a.

The Mössbauer measurements on **2** (295 and 78 K) show a quadrupole-split doublet having an isomer shift $\delta = 0.97$ $mm \cdot s^{-1}$ relative to iron foil and a quadrupole splitting $\Delta E_Q = 2.09$ $mm \cdot s^{-1}$, both parameters being indicative of the +2 high-spin state of the iron.[35,36] When compared to those of other complexes in the lawsone series,[7b] these values are found to be on the lower side, suggesting an increased covalence of the metal-ligand bond resulting probably from d-electron transfer from the non-σ-bonding orbitals of the central atom to the π-acceptor orbitals of corresponding symmetry of the ligand.[37] Such back-donation effects have been observed in other ferrous complexes of hydroxy oxime ligands, which also have a N_2O_4 ligand environment.[38]

The electronic spectrum of **2** in DMF shows a rather broad and asymmetric band at ca. 15 625 cm^{-1}, which probably arises from the mixing-in of the low-intensity component of the d-d transition and the intense charge-transfer band characteristic of metal-quinone compounds.[39]

As a consequence of its dimeric structure, the solubility of **2** in commonly used solvents is very low, resulting in a very weak electroactivity of the solutions. Although it was possible to record the cyclic voltammogram of this complex in DMF with 0.1 M $(C_4H_9)_4NPF_6$ as the supporting electrolyte, it was not possible to extract accurate parameters from the CV profiles. As for the other complexes in the series,[7b] **2** exhibits two cathodic peaks (complex, ca. -650 and -1400 mV; isolated ligand, -844 and -1437 mV) attributable to consecutive one-electron reductions to the semiquinone and catechol anions. The metal ion effect on the electrochemical behavior of the quinone ligand, although weaker, is similar to that observed for the iron(II) complex of the 3-NO_2 derivative.[7b] Finally, although i_{p_c} and i_{p_a} are very low for both observed reductions, both waves are fairly reversible.

Conclusion

Complex **2** has the same $M(L)_2$ general formula as **1** and related ferrous complexes involving other ligands of the lawsone series.[7b] However, while **1** and the parent ferrous complexes include an O_6 ligand environment comprising two bidentate lawsone ligands and two water molecules, the studies described in this paper evidence that the 3-aminolawsone ferrous complex (**2**) includes a N_2O_4 ligand environment involving three aminolawsone ligands and one methanol molecule.

Consequently, **2** exhibits two new characteristics: (i) The coordination sphere of the iron includes a sixth ligand originating from a neighboring complex molecule, which affords antiferromagnetic exchange interactions, as evidenced by the variable-temperature magnetic susceptibility study. (ii) As a consequence of the participation of the C(2) oxygen and C(3) nitrogen atoms

(28) (a) Gill, J. C.; Ivey, P. A. *J. Phys. C: Solid State Phys.* **1974**, *7*, 1536–1550. (b) Kennedy, B. J.; Murray, K. S. *Inorg. Chem.* **1985**, *24*, 1552–1557.

(29) (a) Rudowicz, C. *Acta Phys. Pol.* **1975**, *A47*, 305–321. (b) Champion, P. M.; Sievers, A. J. *J. Chem. Phys.* **1977**, *66*, 1819–1825.

(30) (a) Spiro, C. L.; Lambert, S. L.; Smith, T. J.; Duesler, E. N.; Gagne, R. R.; Hendrickson, D. N. *Inorg. Chem.* **1981**, *20*, 1229–1237. (b) Lambert, S. L.; Hendrickson, D. N. *Inorg. Chem.* **1979**, *18*, 2683–2686. (c) Long, G. L. *Inorg. Chem.* **1978**, *17*, 2702–2707. (d) Tuchagues, J. P.; Hendrickson, D. N. *Inorg. Chem.* **1983**, *22*, 2545–2552. (e) Hartman, J.-A. R.; Rardin, R. L.; Chaudhuri, P.; Phol, K.; Wieghardt, K.; Nuber, B.; Weiss, J.; Papaefthymiou, G. C.; Frankel, R. B.; Lippard, S. J. *J. Am. Chem. Soc.* **1987**, *109*, 7387–7396.

(31) (a) Witteveen, H. T.; Reedijk, J. *J. Solid State Chem.* **1974**, *10*, 151–166. (b) Reem, R. C.; Solomon, E. I. *J. Am. Chem. Soc.* **1987**, *109*, 1216–1226.

(32) Owen, J.; Harris, E. A. In *Electron Paramagnetic Resonance*; Geshwind, S., Ed.; Plenum Press: New York, London, 1972; pp 427–493.

(33) The calculations for an exchange-interacting iron(II) dimer have been carried out in a way similar to that recently described by Reem and Solomon.[31b] Assuming an isotropic exchange interaction, axial zero-field-splitting (D) values equal for the two iron centers, and no rhombic single-ion zero-field splitting ($E_1 = E_2 = 0$), the spin Hamiltonian operator taking into account dipole-dipole interactions (D_i) can be written

$$\mathcal{H} = g_\perp \beta H_\perp [\tfrac{1}{2}(S_1^+ + S_1^- + S_2^+ + S_2^-)] + g_\parallel \beta H_\parallel (S_{z1} + S_{z2}) - 2J[S_{z1}S_{z2} + \tfrac{1}{2}(S_1^+S_2^-) + \tfrac{1}{2}(S_1^-S_2^+)] + D(S_{z1}^2 + S_{z2}^2) + D_i[2S_{z1}S_{z2} - \tfrac{1}{2}(S_1^+S_2^- + S_1^-S_2^+)]$$

In this effective spin Hamiltonian, spin–orbital contributions are taken into account by the D term, while antisymmetric dipole interactions are neglected. By the use of the uncoupled $|S_1S_2\rangle$ basis set, the upper-right triangle nonzero matrix elements reported in the supplementary material are obtained. The molar magnetic susceptibilities are calculated by the classical formula[42]

$$\chi_M = \frac{N}{H} \frac{\sum_i -\partial E_i/\partial H \exp(-E_i/kT)}{\sum_i \exp(-E_i/kT)}$$

The diagonalizations and molar susceptibility calculations are coupled to an adapted version of the STEPT function-minimization procedure.[43]

(34) Supplementary material.

(35) Greenwood, N. N.; Gibb, T. C. *Mössbauer Spectroscopy*; Chapman and Hall: London, 1972; Chapter 6.

(36) Gütlich, P.; Gonser, U., Eds. *Mössbauer Spectroscopy*; Springer-Verlag: New York, 1975; Chapter 2.

(37) Vertes, A.; Tarnoczi, T.; Egyed, C. L.; Papp-Molnar, E.; Burger, K. *Acta Chim. Hung.* **1969**, *59*, 19–22.

(38) Burger, K.; Korecz, L.; Manuaba, I. B. A.; Mag, P. *J. Inorg. Nucl. Chem.* **1966**, *28*, 1673–1678.

(39) Wicklund, P. A.; Brown, D. G. *Inorg. Chem.* **1976**, *15*, 396–400.

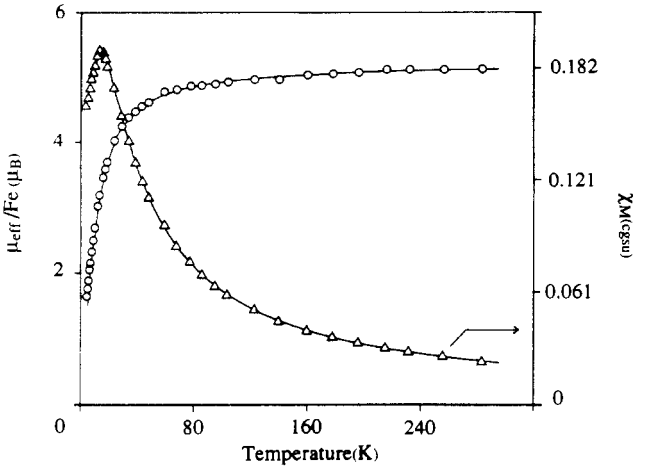

Figure 4. Variable-temperature magnetic susceptibility data for [Fe(3-aminolawsonato)$_2$(CH_3OH)]. The solid lines result from a least-squares fit of the data to the theoretical magnetic susceptibility calculated by exact diagonalization of the effective spin Hamiltonian taking into account the single-ion and dipolar ZFS terms.[33,34]

in the coordination to the ferrous iron, both carbonyl functions of the 3-aminolawsone ligand are not directly involved in the coordination to the ferrous center. As evidenced in Figure 3, this new structural arrangement holds the carbonyl functions of two *p*-naphthoquinones at ca. 4 Å from a ferrous center, thus affording the best structural analogue of the ferroquinone complex of photosynthetic bacteria[40] described up to now. In view of the unsuccessful attempts to synthesize ferrous complexes of quinonoid ligands in the past, wherein high-spin iron(III) compounds were obtained,[30,41] the present work provides structural and physicochemical data on stable iron(II) complexes containing two quinonoid ligands. It can, therefore, serve as a basis for studying the effect of quinone oxidation state changes on electronic and magnetic properties of the iron(II)–quinone couple in photosynthetic reaction centers.

Acknowledgment. We thank Dr. M. P. Gupta, National Chemical Laboratory, Poona, India, Dr. S. K. Kulshrestha, Chemistry Division, BARC, Bombay, India, and Dr. V. Petroulêas, NRC DEMOKRITOS, Athens, Greece, for the Mössbauer measurements. J. Aussoleil is thanked for valuable discussions concerning the computational details of the magnetic susceptibility calculations. We are indebted to M. A. Martinez Lorente for devising an accurate purification method for the 3-aminolawsone ligand. The financial assistance from DNES and CNRS (ATP Photosynthêse and ARI Chimie-Biologie) is gratefully acknowledged. This work has been partially developed within the framework of the CNRS/CSIR exchange program.

Supplementary Material Available: Figure 5, showing a stereoview of complex **1** along [100], Tables IV–VI, listing crystallographic data, final non-hydrogen thermal parameters, and deviations of atoms from their least-squares planes for complex **1**, respectively, Table VIII, listing the experimental magnetic susceptibility data for complex **2**, and Table IX, listing the upper-right triangle nonzero matrix elements obtained in the solution of the spin Hamiltonian of ref 33 in the uncoupled $|S_1S_2\rangle$ basis set (11 pages); Table VII, listing the observed and calculated structure factor amplitudes for complex **1** (8 pages). Ordering information is given on any current masthead page.

(40) (a) Deisenhofer, J.; Epp, O.; Miki, K.; Huber, R.; Michel, H. *J. Mol. Biol.* **1984**, *180*, 385–398. (b) Deisenhofer, J.; Epp, O.; Miki, K.; Huber, R.; Michel, H. *Nature* **1985**, *318*, 19–26. (c) Michel, H.; Epp, O.; Deisenhofer, J. *EMBO J.* **1986**, *5*, 2445–2451. (d) Allen, J. P.; Feher, G.; Yeates, T. O.; Rees, D. C.; Deisenhofer, J.; Michel, H.; Huber, R. *Proc. Natl. Acad. Sci. U.S.A.* **1986**, *84*, 5730–5734. (e) Allen, J. P.; Feher, G.; Yeates, T. O.; Rees, D. C. *Proc. Natl. Acad. Sci. U.S.A.* **1987**, *84*, 5730–5734. (f) Allen, J. P.; Feher, G.; Yeates, T. O.; Komiya, H.; Rees, D. C. *Proc. Natl. Acad. Sci. U.S.A.* **1988**, *85*, 8487–8491.

(41) (a) Buchanan, R. M.; Downs, H. H.; Shorthill, W. B.; Pierpont, C. G.; Kessel, S. L.; Hendrickson, D. N. *J. Am. Chem. Soc.* **1978**, *100*, 4318–4320. (b) Kessel, S. L.; Hendrickson, D. N. *Inorg. Chem.* **1978**, *17*, 2630–2636. (c) Kessel, S. L.; Hendrickson, D. N. *Inorg. Chem.* **1980**, *19*, 1883–1889. (d) Lynch, M. W.; Valentine, M.; Hendrickson, D. N. *J. Am. Chem. Soc.* **1982**, *104*, 6982–6989.

(42) See, for example: Laskowski, E. J.; Hendrickson, D. N. *Inorg. Chem.* **1978**, *17*, 457–470.

(43) Chandler, J. P. Quantum Chemistry Program Exchange, Indiana University; Program 66.